Mine Water and the Environment (2021) 40:539–546
https://doi.org/10.1007/s10230-020-00747-x

TECHNICAL ARTICLE

Fast Fisher Discrimination of Water-Rich Burnt Rock Based on DC Electrical Sounding Data

Haijun Xie[1] · Jin Li[1] · Yi Dong[2] · Gongyu Li[3] · Zihao Han[4]

Received: 23 January 2020 / Accepted: 15 December 2020 / Published online: 4 February 2021

Abstract
Direct current (DC) electrical sounding was performed to quickly identify the location of potentially dangerous water hidden in burnt rock (formed by spontaneous combustion of the coal). The Fisher discriminant method was used to generate the functional relationship between borehole water inflow and DC electrical sounding data, and a model was established to identify the water-enriched burnt rock areas. Based on a reevaluation of the training samples, the accuracy of the water-rich discrimination model was found to be 89.1%. Finally, the water enrichment in the burnt area was predicted based on DC sounding data from 576 survey points in five exploration lines, and the predictions were compared with the subsequent water inflow data from boreholes. We found that the predicted results were highly consistent with the water inflow data in the boreholes. Thus, the feasibility of using this approach was verified.

Keywords DC sounding · Burnt rock water enrichment property · Fisher discrimination · Mine water management

Introduction

Safe and efficient production in coal mines requires the application of advanced geophysical technologies to accurately detect the locations of water-rich areas, as well as concealed water diversion channels (Xue et al. 2018, 2019). Electrical and electromagnetic methods have become the main means by which hydrogeological investigations and deep explorations are conducted in mined-out areas (Chen et al. 2019a, b).

Spontaneous combustion of coal seams can transform the rock formation above the coal into burnt rock; the resultant void space, if filled with water, can seriously threaten safety during coal mine production (Hou et al. 2017; Yue and Xue 2016). Hence, the distribution of the water-enriched burnt rock above a working face must be clearly detected before extraction.

The traditional detection method involves the use of electrical resistivity. However, most resistivity inversions used at present adopt a uniform half-space model to perform qualitative interpretation. Furthermore, many initial input parameters are needed during the inversion of a stratified model, and there are additional model and algorithm requirements (Chen et al. 2017; Pan and Tang 2014; Thomas et al. 2006; Wang et al. 2011; Zhang et al. 2016). Also, the multi-dimensional inversion theory is complex and time-consuming with respect to computation, and when it is used, it is often difficult to reflect the real strata, particularly, in areas for which geological data is lacking. Without a reference base for the selection and delineation of the range of the threshold resistivity value in a water-enriched zone, it is difficult to make a reasonable geological interpretation for the inverted low resistance anomaly (Cheng and Shi 2013; Elwaseif et al. 2012; Gao et al. 2018; Liu et al. 2014; Loke et al. 2013; Lu et al. 2017; Thomas et al. 2006; Yue and Xue 2016). Therefore, based on the application of Fisher discrimination in seismic exploration (Chen et al. 2016; Dong et al. 2016), Fisher discrimination was used in this study to avoid the above-mentioned complicated theoretical calculations.

✉ Jin Li
18789436885@163.com

[1] College of Geology and Environment, Xi'an University of Science and Technology, Xi'an 710054, China

[2] College of Geoscience and Surveying Engineering, China University of Mining & Technology (Beijing), Beijing 100083, China

[3] Xi'an Researcher Institute Co. Ltd., China Coal Technology and Engineering Group Corp., Xi'an 710077, China

[4] Geotech Ltd, 270 Industrial Pkwy S, Aurora, ON L4G 3T9, Canada

There are several studies on the use of Fisher discrimination to hydrogeological conditions in China. For example, Dong and Xie (2016) selected seven hydrochemical indicators that can be used to distinguish water source types and established the Fisher discrimination model for the water inrush source in 32 blocks in the Xu Tuan Mine; the model exhibited high discrimination accuracy. Hou et al. (2016) using evaluation indices such as thickness and weathering degree of the bedrock, established a Fisher prediction model for the water enrichment of the weathered bedrock of Jurassic coalfield in north Shaanxi, and verified the feasibility of the model. Zhang et al. (2013) used indicators such as fault transmissibility and tectonic development to establish a Fisher model for water inrush risk in the seam floor, and applied and tested the model in the Panxi Mine. However, these and similar studies are only mathematical models established based on geological indices. So far, no study using the Fisher discrimination model based on geophysical exploration methods has been reported.

In this study, direct current (DC) sounding data, borehole water inflow data, and the Fisher mathematical model, as well as normalized voltage reflecting the difference in strata water enrichment were combined as indices to establish a discrimination model for burnt rock water enrichment. This study also provides a reference for the processing of other electrical exploration data types.

Principles of Fisher Discrimination

Statistical methods usually transform high-dimensional space data into low-dimensional space data to establish a model. Fisher discrimination projects multi-dimensional data in a particular direction (Hu et al. 2010; Pan 2013; Zhao 2012):

$$\mathrm{y} = a_1x_1 + a_2x_2 + \ldots\ldots + a_nx_n = w^TX \tag{1}$$

where X represents a selected variable that can reflect the object under study, w^T expresses a coefficient to be determined, and y represents the discrimination value.

$$\overline{\mathrm{y}} = \frac{1}{n}\sum y \tag{2}$$

$$\overline{\mathrm{y}}_i = \frac{1}{n_i}\sum_{y_k \in Y_i} y_k,\ i = 1, 2, 3 \ldots\ldots \tag{3}$$

where $\overline{\mathrm{y}}$ represents the mean value of all the discrimination values, $\overline{\mathrm{y}}_i$ expresses the mean value of different sets of discrimination values, Y_i expresses the ensemble of different sets, and y_k expresses the discrimination value of each set.

$$S_{\mathrm{i}}^2 = \sum_{y_k \in Y_i} (y_k - \overline{\mathrm{y}}_i)^2,\ i = 1, 2, 3 \ldots\ldots \tag{4}$$

Here, S_{i}^2 expresses the dispersion inside a set, i.e. variance. The system of linear equations is established based on the known sample types. The difference between different sample point types is enlarged as much as possible, and simultaneously, the difference between similar sample point types is reduced as much as possible. Thus, the Fisher criterion function is defined as:

$$J_F(W) = \frac{\sum_{i=1}^{n} n_{\mathrm{i}}[\overline{y}_i - \overline{y}]^2}{\sum_{i=1}^{n} S_i^2} \tag{5}$$

To make the maximum coefficient matrix, w, of $J_F(W)$, the vector of optimum solution, i.e. the coefficient of the different variables in the Fisher linear discrimination formula, formulas (1), (2), (3), (4) and (5) are then combined to construct a Lagrange function. Following establishment of the discrimination model, training samples are selected to perform back evaluation to estimate the accuracy of the model, based on the ratio of the number of the correct samples from the back evaluation to the total number of samples, denoted as η.

Establishment of the Fisher Model

Methods of Data Collection and Research

An uncommon burnt zone, with an area of 1.6 km^2, had developed in seam 1–2 upper at the south wing of a coal mine in north Shaanxi, in northwest China. Based on the area's geological features, it was speculated that it contained an unevenly distributed amount of water. The drilling data indicated the presence of a relatively water-enriched weathered layer in the bedrock above the coal seam. The hydraulic connection formed by the fractures in the burnt rock and the weathered layer of the bedrock constituted a serious threat to safe mining of the underlying coal seam. Hence, learning the distribution of the water enrichment property of the burnt rock was essential. Figure 1 presents a flow diagram of the study area. Based on a comprehensive consideration of various factors, the water enrichment of the study area was surveyed using a tri-electrode DC electrical sounding arrangement. The measurement grid was arranged as shown in Fig. 2. In combination with the actual geological conditions, five survey lines were laid in the burnt area and its vicinity. The survey points were 15 m apart and a total of 567 survey points were considered. Data were collected in the depth direction at each survey point, and a total of 20 depth levels were considered, with the maximum theoretical depth being 300 m.

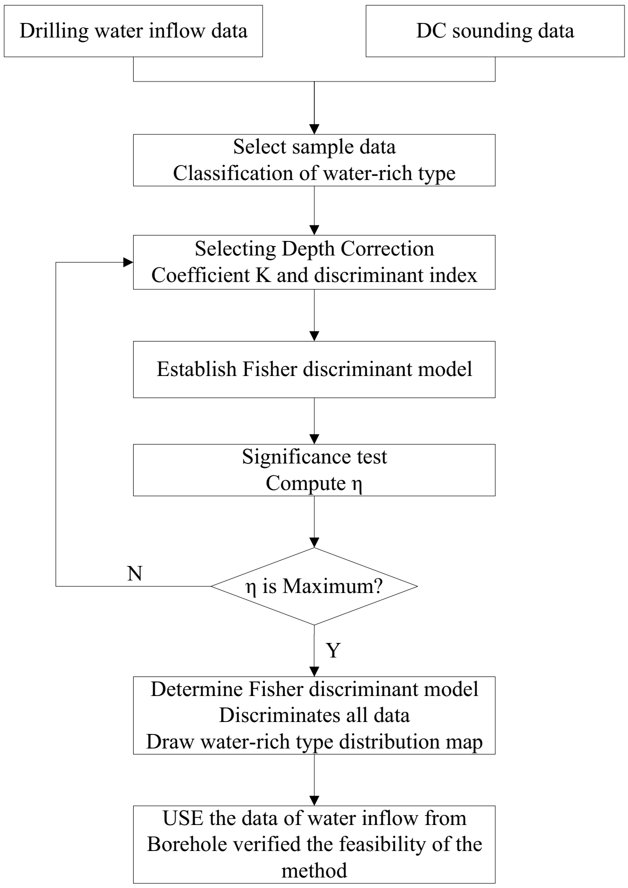

Fig. 1 Flow diagram of the study

Principle of Index Selection

The location and range of the horizons where the burnt rock was located were determined based on existing drilling data, in combination with water inflow data from where the burnt area exposed by hydrological boreholes, and the area's actual geological situation. The water enrichment aspect of the area was artificially divided into three types: moderate water enrichment (0.1 L/(s m) < q < 1 L/(s m)), slight water enrichment (q < 0.1 L/(s m)), and very slight water enrichment (q < 0.01 L/(s m)). Drilling data in the study area showed that the burial depth of the burnt area was 125 m; therefore, the data in the vicinity of the burial depth of 125 m was selected as a variable for the model. Due to the volume effect of the DC electrical method, low resistance abnormal bodies usually cause nearby surrounding areas to show relatively low resistivity. In combination with the known position of the burnt rock exposed by the boreholes, the normalized electromotive force V/I of five sets of electrical sounding data corresponding to the burnt area above and below the burial depth of 125 m were selected as the discrimination indices, i.e. the sounding performed at 90, 105, 120, 135, and 150 m, were marked as X_1, X_2, X_3, X_4, and X_5, respectively. 55 DC electrical sounding measurement points, with different water enrichment levels, and 11 existing boreholes (six with medium water enrichment, three with simple water enrichment, and two with very simple water enrichment) were selected as training samples to establish the model. These were divided into sample groups according to water inflow.

For correction, it is often necessary to multiply the actual depth obtained using the DC electrical method in the field by a suitable coefficient, *K*. In the past, the practice was to search for a marker bed and use the inversion profile of the apparent resistivity for the determination of the coefficient, *K*.

$$H = K * OA \tag{6}$$

where *H* represents the actual detection depth and *OA* represents the interval of the power supply electrode. In this study, the Fisher discrimination models were set up by selecting the correction coefficient, *K*, at different depths; the model with the highest back evaluation accuracy was selected as the final model. The accuracy of the back evaluation of different coefficients is shown in Table 1; the accuracy was highest when *K* was 0.75. Table 2 shows the results of the back evaluation for the 55 training samples.

Establishment of the Fisher Model Discrimination Equation

The coefficient of the discrimination function obtained based on the data corresponding to the selected samples and with the help of SPSS software (version 19), i.e. the vector coefficient matrix of the optimum solution, is presented in Table 3.

$$y_1 = 0.563x_1 + 0.816x_2 - 1.054x_3 - 0.448x_4 + 0.959x_5 \tag{7}$$

$$y_2 = -0.134x_1 + 1.334x_2 - 0.109x_3 + 0.263x_4 - 1.149x_5 \tag{8}$$

These formulas are the discriminant functions for the three types of water enrichment, where x_1–x_5 represents V/I at a depth in the range 135–195 m, and y_1 and y_2 represent the Fisher discriminant equations. The above model is the Fisher model set-up when $K = 0.75$.

Back Evaluation of the Training Samples of the Fisher Model

According to the Fisher discrimination principle, data corresponding to the training samples were substituted into formulas (7) and (8) of the established Fisher model, y_1 and y_2 were calculated, and the results obtained were compared with the center position of each group and grouped with the group's result closest to the projection position. From Table 2, it is evident that among the 55 training samples,

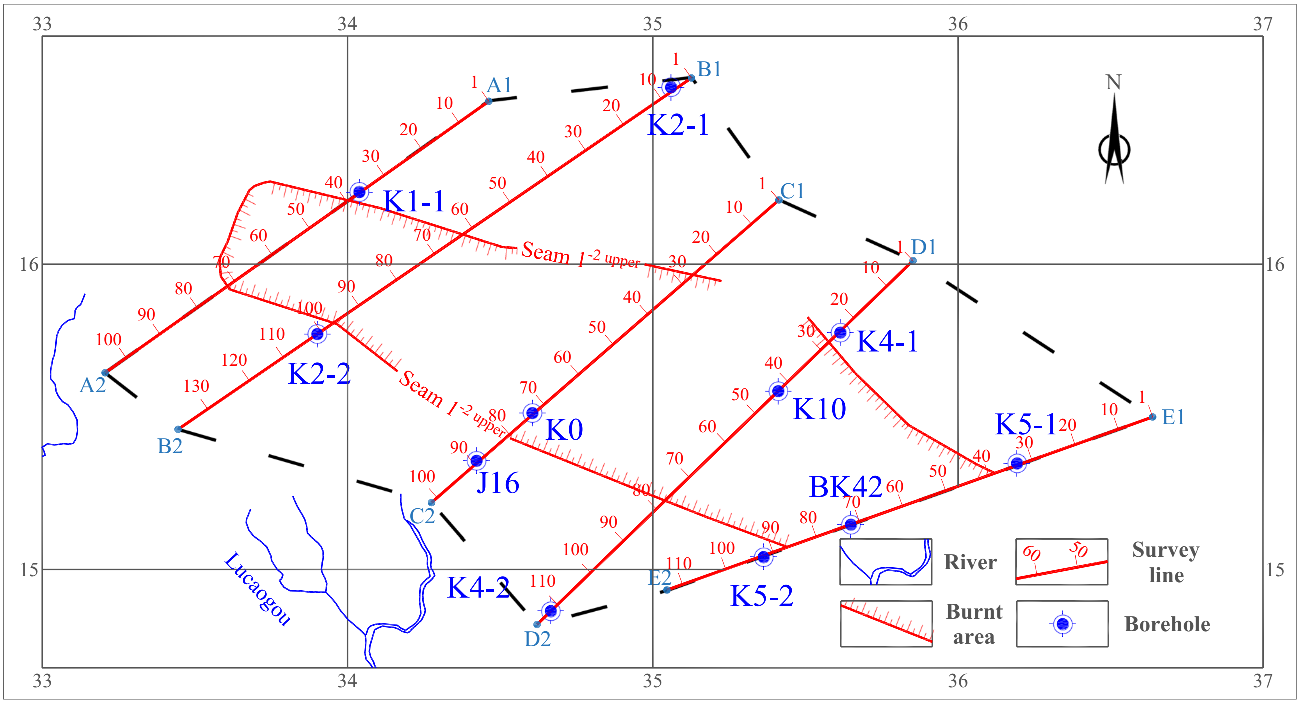

Fig. 2 Layout of the survey grid and borehole distribution in the study area

only six samples (samples 20, 36, 38, 44, 45, and 50) had an incorrect water enrichment type. All the other samples had water enrichment identical to the actual classification, with an accuracy up to 89.1%. This illustrates that the established model was highly accurate in discriminating water enrichment in the study area. The incorrect discrimination observed during the back evaluation of the training samples could have been caused by the potential difference decreasing rapidly during field data acquisition as the exploration depth increased, resulting in a decreased signal-to-noise ratio (SNR). This possibly led to the distortion of the deeper data.

Figure 3 shows a grouping diagram drawn by applying the discriminant functions, y_1 and y_2. From this figure, it can be observed that the water enrichment types overlapped at some points. This could result in incorrect discrimination of the samples projected onto the junction during the back evaluation of the Fisher model. In addition, during the selection of training samples, hydrological drilling data were used as a criterion; hence, statistical errors in the drilling depth could have influenced the selection of the training samples. Nonetheless, the discrimination method used in this study is simple, was highly accurate, and could discriminate the water enrichment at the survey point locations as long as the original electrical sounding record of the different survey points is known.

Table 1 Accuracy of back evaluation of samples for correction coefficient of different depths

K	η (%)	K	η (%)
1	81.8	0.9	81.8
0.8	83.6	0.75	89.1
0.7	87.3	0.65	83.6
0.6	80	0.55	80
0.5	81.8		

Discrimination of Water Enrichment in the Study Area

Following categorization of the DC electrical sounding data acquired in the field and on the basis of the Fisher discriminant model established in this study, the levels of water enrichment at the 567 survey points in the study area were discriminated. It was observed that 364, 102, and 101 of the survey points corresponded to Type I, Type II, and Type III water enrichment types, respectively. Figure 4 shows the water enrichment distribution based on this prediction.

Based on known hydrogeological data, the groundwater is mainly derived from runoff that flows into the Lucaogou gully on the southwestern side of the study area. moving to the southwest from the northeast. Therefore, water enrichment was found to be relatively strong in the southwestern portion of the study area and relatively weak in the northeast. Prediction diagram 3 shows that, overall, the water enrichment in the southwest of the study area was stronger than in the northeast, coinciding with the hydrogeological situation. Notably, during the selection of the training samples, boreholes K1-2, K3, K9 and

Table 2 Comparison of training samples for back evaluation of strong/weak water enrichment and the results of self-inspection

Sample	No of survey point	No of borehole	Unit water inflow L/(s m)	Normalized electromotive force (mV/A) of different depth					Actual classification	Fisher Back evaluation
				120 m	135 m	150 m	165 m	180 m		
1	E-69	BK42	0.125	10.533	8.839	7.996	6.949	6.279	I	I
2	E-70	BK42	0.125	11.051	9.320	8.054	7.154	6.555	I	I
3	E-71	BK42	0.125	10.924	9.172	7.962	7.194	6.285	I	I
4	E-72	BK42	0.125	11.742	9.730	8.506	7.614	6.786	I	I
5	E-73	BK42	0.125	13.288	11.002	9.565	8.571	7.816	I	I
6	C-86	J16	0.125	10.715	8.982	7.659	6.979	6.128	I	I
7	C-87	J16	0.125	11.300	9.396	8.177	7.118	6.591	I	I
8	C-88	J16	0.125	10.014	8.453	7.237	6.480	5.794	I	I
9	C-89	J16	0.125	9.917	8.541	7.419	6.519	6.034	I	I
10	C-90	J16	0.125	10.843	9.081	8.012	7.158	6.435	I	I
11	C-68	K0	0.004	15.126	12.392	10.502	9.157	8.419	III	III
12	C-69	K0	0.004	16.119	13.037	11.380	10.141	8.815	III	III
13	C-70	K0	0.004	16.001	13.437	11.665	10.288	9.070	III	III
14	C-71	K0	0.004	14.278	11.961	10.231	8.746	7.895	III	III
15	C-72	K0	0.004	13.803	11.870	10.205	9.087	8.262	III	III
16	D-40	K10	0.038	14.937	12.367	20.450	9.397	8.544	II	II
17	D-41	K10	0.038	22.257	16.584	13.187	11.714	11.806	II	II
18	D-42	K10	0.038	25.323	21.062	18.611	15.473	13.826	II	II
19	D-43	K10	0.038	20.473	16.207	13.648	11.792	10.791	II	II
20	D-44	K10	0.038	13.434	11.367	10.065	8.910	8.000	II	I*
21	A-33	K1-1	0.162	9.086	7.724	6.473	5.808	5.315	I	I
22	A-34	K1-1	0.162	10.196	8.393	7.022	6.523	5.782	I	I
23	A-35	K1-1	0.162	10.121	8.352	7.405	6.382	5.754	I	I
24	A-36	K1-1	0.162	7.957	6.829	5.812	5.119	4.642	I	I
25	A-37	K1-1	0.162	12.495	10.172	8.796	7.796	6.995	I	I
26	B-4	K2-1	0.121	10.625	9.160	7.897	7.037	6.423	I	I
27	B-5	K2-1	0.121	7.966	6.485	5.436	4.868	4.250	I	I
28	B-6	K2-1	0.121	8.101	6.481	5.702	4.876	4.475	I	I
29	B-7	K2-1	0.121	12.347	10.335	9.000	7.941	6.892	I	I
30	B-8	K2-1	0.121	12.812	10.994	9.574	8.584	7.717	I	I
31	B-100	K2-2	0.241	11.936	9.873	8.239	7.241	6.691	I	I
32	B-101	K2-2	0.241	17.649	12.530	9.750	8.194	7.313	I	I
33	B-102	K2-2	0.241	15.235	12.568	9.029	7.631	6.763	I	I
34	B-98	K2-2	0.241	13.328	10.780	9.210	7.250	6.065	I	I
35	B-99	K2-2	0.241	11.407	9.097	7.650	6.709	5.553	I	I
36	D-21	K4-1	0.004	13.293	21.995	9.499	8.462	7.620	III	II*
37	D-22	K4-1	0.004	14.977	12.675	10.958	9.608	8.599	III	III
38	D-23	K4-1	0.004	13.590	11.115	9.842	8.816	8.066	III	I*
39	D-24	K4-1	0.004	16.083	13.597	11.403	10.446	9.645	III	III
40	D-25	K4-1	0.004	13.565	11.454	9.903	8.629	8.041	III	III
41	D-109	K4-2	0.110	10.563	9.057	7.887	7.073	6.525	I	I
42	D-110	K4-2	0.110	11.841	10.220	8.822	7.611	6.741	I	I
43	D-111	K4-2	0.110	10.885	15.714	19.133	25.340	10.382	I	I
44	D-112	K4-2	0.110	12.572	10.693	9.182	8.149	7.368	I	III*
45	D-113	K4-2	0.110	13.979	12.008	10.343	9.186	8.146	I	III*
46	E-30	K5-1	0.081	19.454	14.928	12.925	11.370	10.232	II	II
47	E-31	K5-1	0.081	17.315	13.281	11.374	9.614	1.242	II	II

Table 2 (continued)

Sample	No of survey point	No of borehole	Unit water inflow L/(s m)	Normalized electromotive force (mV/A) of different depth					Actual classification	Fisher Back evaluation
				120 m	135 m	150 m	165 m	180 m		
48	E-32	K5-1	0.081	22.204	18.308	14.856	12.096	10.470	II	II
49	E-33	K5-1	0.081	20.776	15.535	12.815	11.301	10.153	II	II
50	E-34	K5-1	0.081	16.028	13.350	11.389	10.113	9.255	II	III*
51	E-89	K5-2	0.084	20.649	16.496	13.868	12.333	11.122	II	II
52	E-90	K5-2	0.084	25.325	19.146	15.840	13.759	12.426	II	II
53	E-91	K5-2	0.084	22.481	16.215	13.052	11.270	10.009	II	II
54	E-92	K5-2	0.084	20.489	16.003	12.276	10.275	9.162	II	II
55	E-93	K5-2	0.084	23.776	17.622	14.473	11.756	10.256	II	II

*The classification with asterisk represents that it did not coincide to the actual classification, in the table, I is medium water enrichment, II is simple water enrichment and III is very simple water enrichment

Table 3 Standardized canonical discriminant function coefficients

Variable	Function	
	y_1	y_2
x_1	0.563	−0.134
x_2	0.816	1.334
x_3	−1.054	−0.109
x_4	−0.448	0.263
x_5	0.959	−1.149

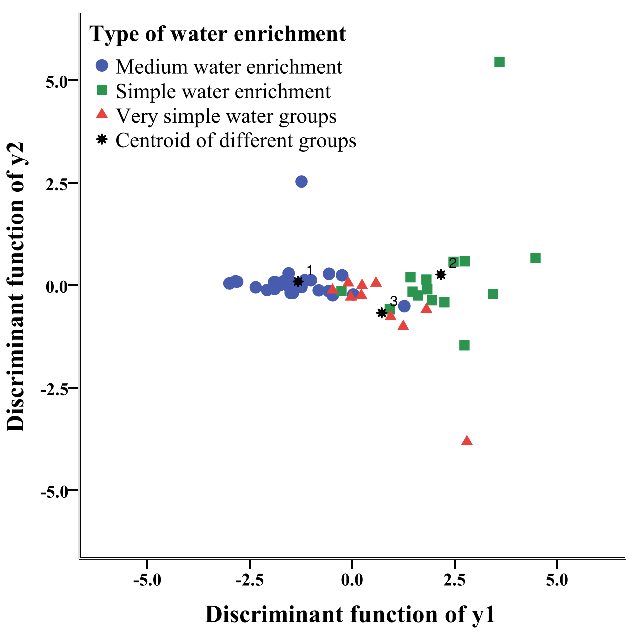

Fig. 3 Grouping of discriminant function of y1 and y2

BK38, were not selected, and of these, K9 was located in the burnt area. The results of the pumping test of the four boreholes were as follows: K1-2 showed slight water enrichment, K9 showed moderate water enrichment, and BK38 and K3 showed very slight water enrichment (the columnar sections of the boreholes are shown in Fig. 5). The water enrichment of the above boreholes was consistent with the discrimination in the prediction diagram. This indicated that the original DC electrical sounding data could be practically and effectively applied to establish the Fisher discriminant model and accurately predict the water enrichment in the entire area.

Conclusions

In this study, we established a Fisher discriminant model to discriminate the water enrichment in a coal mine, based on selected data samples. The accuracy of the back evaluation of the samples using the model reached 89.1%, showing that the model could be applied to discriminate the water enrichment types in the study area.

Additional training samples for subsequent drilling verification could be added to improve the model. This could be done by comparing and selecting the back-estimation accuracy, η, of the discrimination model established based on different depth coefficients, *K*, to correct the exploration depth of the DC sounding method.

The Fisher discriminant model was established based on DC electric sounding data and borehole water inflow

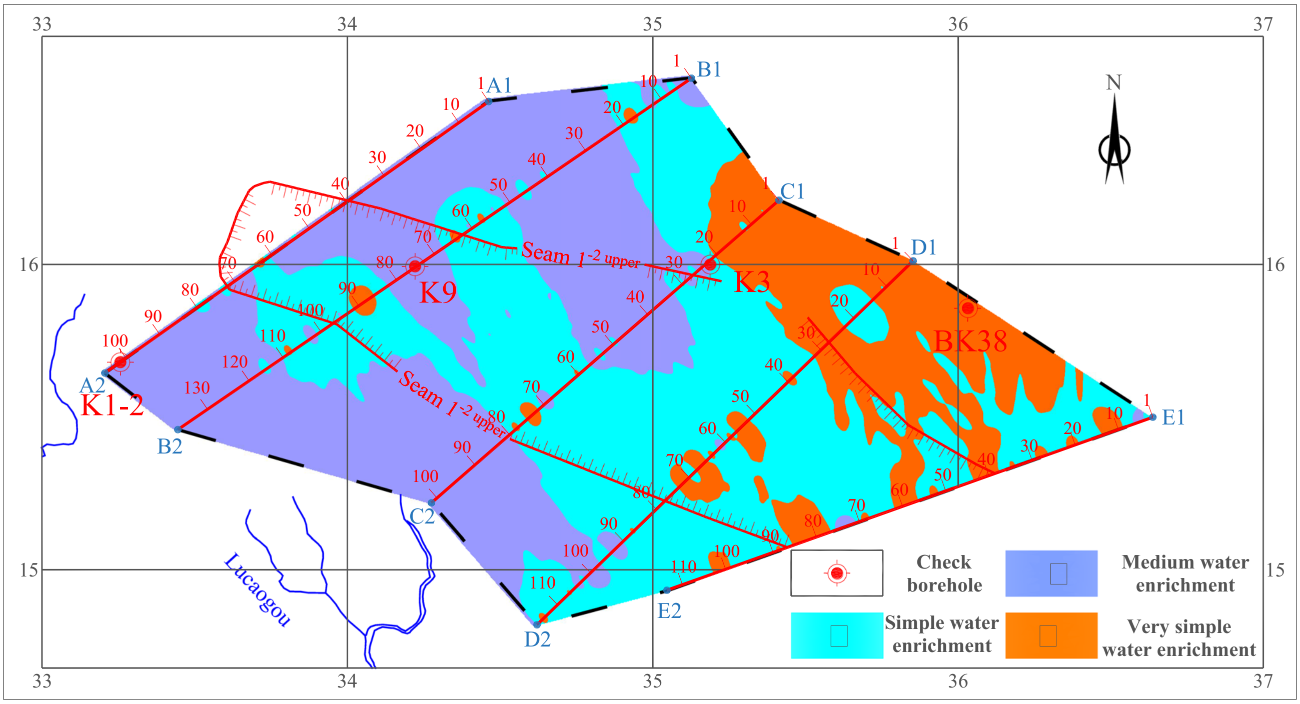

Fig. 4 Prediction of distribution of water enrichment types in the study area

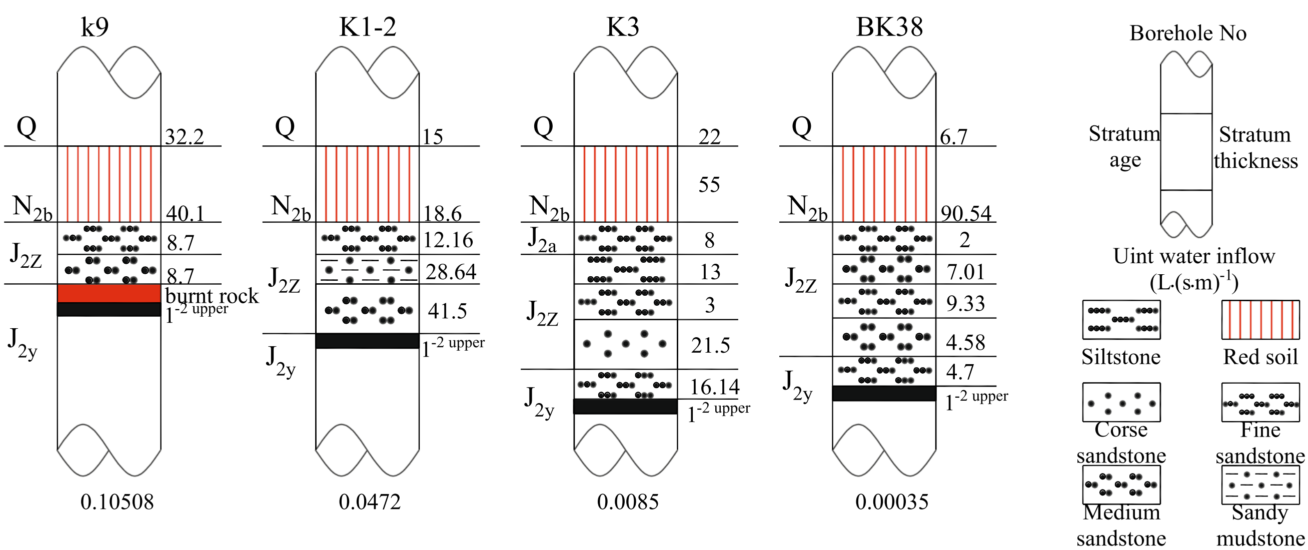

Fig. 5 Histogram of pumping test boreholes

data. This method can be used elsewhere for water disaster prevention and control in coal mines. Original data from other electromagnetic exploration methods can also be used for interpretations. Considering that the accuracy of the model requires original geophysical data of high quality, this discriminant method is suitable for study areas with simple geological conditions and little interference.

Acknowledgements The authors thank the National Natural Science Foundation for funding this research (Grant 41472234). We also thank Editage for English language editing.

References

Chen WH, Dong SQ, Wang ZZ, Hou JG, Li HL (2016) Seismic reservoir quality evaluation in tight sandstone reservoirs. J China Univ Pet Ed Nat Sci 40(3):68–68. https://doi.org/10.3969/j.issn.1673-5005.2016.03.008 (**in Chinese**)

Chen H, Deng JZ, Yin M, Yin CC, Tang WW (2017) Three-dimensional forward modeling of DC resistivity using the aggregation-based algebraic multigrid method. Appl Geophys 14(1):154–164. https://doi.org/10.1007/s11770-017-0605-1

Chen K, Xue GQ, Chen WY, Zhou NN, Li H (2019a) Fine and quantitative evaluations of the water volumes in an aquifer above the coal seam roof, based on TEM. Mine Water Environ 38(1):49–59. https://doi.org/10.1007/s10230-018-00573-2

Chen K, Zhang JY, Xue GQ, Huang H, Chen WY, Hao JT, Yue YZ (2019b) Feasibility of monitoring hydraulic connections between aquifers using time-lapse TEM: a case history in inner Mongolia, China. J Environ Eng Geophys 24(3):361–372. https://doi.org/10.2113/jeeg24.3.361

Cheng JY, Shi XX (2013) Current status and development of coal geophysical technology in China. Prog Geophys 28(4):2024–2032. https://doi.org/10.6038/pg20130446 (**in Chinese**)

Dong Y, Xie HJ (2016) Discrimination analysis of water inrush source by Fisher in Xutuan mine 32 block. J Xi'an Univ Sci Technol 36(1):79–83. https://doi.org/10.13800/j.cnki.xakjdxxb.2016.0113 (**in Chinese**)

Dong LJ, Wesseloo J, Potvin Y, Li XB (2016) Discrimination of mine seismic events and blasts using the Fisher Classifier, naive Bayesian Classifier and logistic regression. Rock Mech Rock Eng 49(1):183–211. https://doi.org/10.1007/s00603-015-0733-y

Elwaseif M, Ismail A, Abdalla M, Abdel-Rahman M, Hafez MA (2012) Geophysical and hydrological investigations at the west bank of Nile River (Luxor, Egypt). Environ Earth Sci 67(3):911–921. https://doi.org/10.1007/s12665-012-1525-2

Gao WF, Shi LQ, Han J, Zhai PH (2018) Dynamic monitoring of water in a working face floor using 2D electrical resistivity tomography (ERT). Mine Water Environ 37(3):423–430. https://doi.org/10.1007/s10230-017-0483-z

Hou EK, Tong RJ, Wang SJ, Feng J, Chen T (2016) Prediction method for the water enrichment of weathered bedrock based on Fisher model in northern Shaanxi Jurassic coalfield. J China Coal Soc 41(9):2312–2318. https://doi.org/10.13225/j.cnki.jccs.2016.0240 (**in Chinese**)

Hou EK, Tong RJ, Feng J, Che XY (2017) Water enrichment characteristics of burnt rock and prediction on water loss caused by coal mining. J China Coal Soc 42(01):175–182. https://doi.org/10.13225/j.cnki.jccs.2016.5055 (**in Chinese**)

Hu HH, Liu Z, Li ZJ, Cui TT (2010) Fisher discriminant analysis to the classification of spontaneous combustion tendency grade of sulphide ores. J China Coal Soc 35(10):1674–1679. https://doi.org/10.13225/j.cnki.jccs.2010.10.029 (**in Chinese**)

Liu SD, Liu J, Yue JH (2014) Development status and key problems of Chinese mining geophysical technology. J China Coal Soc 39(1):19–25. https://doi.org/10.13225/j.cnki.jccs.2013.0587 (**in Chinese**)

Loke MH, Chambers JE, Rucker DF, Kuras O, Wilkinson PB (2013) Recent developments in the direct-current geoelectrical imaging method. J Appl Geophys 95:135–156. https://doi.org/10.1016/j.jappgeo.2013.02.017

Lu T, Liu SD, Wang B, Wu RX, Hu XW (2017) A review of geophysical exploration technology for mine water disaster in China: applications and trends. Mine Water Environ 36(3):1–10. https://doi.org/10.1007/s10230-017-0467-z

Pan JS (2013) Fisher's discriminant analysis and application. Pract Underst Math 43(05):155–162. https://doi.org/10.3969/j.issn.1000-0984.2013.05.024 (**in Chinese**)

Pan KJ, Tang JT (2014) 2.5-D and 3-D DC resistivity modelling using an extrapolation cascadic multigrid method. Geophys J Int 197(3):1459–1470. https://doi.org/10.1093/gji/ggu094

Thomas G, Carsten R, Klaus S (2006) Three-dimensional modelling and inversion of DC resistivity data incorporating topography – I. Model Geophys J Int 166(2):495–505. https://doi.org/10.1111/j.1365-246X.2006.03011.x

Wang XL, Feng H, Tian HG, Wu D (2011) Direct current forward modeling based on COMSOL MULTIPHYSICS. Coal Geol Explor 39(05):79–83. https://doi.org/10.3969/j.issn.1001-1986.2011.05.019 (**in Chinese**)

Xue GQ, Hou DY, Qiu WZ (2018) Identification of double-layered water filled zones using TEM: a case study in China. J Environ Eng Geophys 23(3):297–304. https://doi.org/10.2113/JEEG23.3.297

Xue GQ, Chen W, Cheng JL, Liu SC, Yu JC, Lei KX, Guo WB, Feng XH (2019) A review of electrical and electromagnetic methods for coal mine exploration in China. IEEE Access. https://doi.org/10.1109/ACCESS.2019.2951774

Yue JH, Xue GQ (2016) Review on the development of Chinese coal electric and electromagnetic prospecting during past 36 years. Prog Geophys 31(4):1716–1724. https://doi.org/10.6038/pg20160441 (**in Chinese**)

Zhang WQ, Zhang GP, Li W, Hua X (2013) A model of Fisher's discriminant analysis for evaluating water inrush risk from coal seam floor. J China Coal Soc 38(10):1831–1836. https://doi.org/10.13225/j.cnki.jccs.2013.10.027 (**in Chinese**)

Zhang QJ, Dai SK, Chen LW, Qiang JK, Li K, Zhao DD (2016) Finite element numerical simulation of 2.5D direct current method based on mesh refinement and recoarsement. Appl Geophys 13(2):257–266. https://doi.org/10.1007/s11770-016-0562-0

Zhao LN (2012) The study on introduction weighting factor of fisher discriminant. Nat Sci J Harbin Norm Univ 28(5):24–26. https://doi.org/10.3969/j.issn.1000-5617.2012.05.009 (**in Chinese**)